

Topological self-dual configurations in a Lorentz-violating gauged $O(3)$ sigma model

R. Casana,^{*} C. F. Farias,[†] and M. M. Ferreira, Jr.[‡]

Departamento de Física, Universidade Federal do Maranhão, 65080-805 São Luís, Maranhão, Brazil.

We have studied the existence of topological Bogomol'nyi-Prasad-Sommerfield or self-dual configurations in a Lorentz-violating gauged $O(3)$ nonlinear sigma model, where CPT -even Lorentz-violating (LV) terms were introduced in both the gauge and σ -field sectors. As happens in the usual gauged σ model, purely magnetic self-dual configurations are allowed, maintaining some qualitative features of the standard ones. In a more involved configuration, Lorentz violation provides new self-dual magnetic solutions carrying an electric field but a null total electric charge. In both cases, the total energy of the self-dual configurations turns out to be proportional to the topological charge of the model and to the LV parameters introduced in the σ sector. It is shown that the LV terms yield magnetic flux reversion as well.

I. INTRODUCTION

In condensed matter physics, Abrikosov's description for type-II superconductors [1] has led to an increasing interest in the study of magnetic flux vortices that naturally stem from Ginzburg-Landau theory [2]. In field theory, stable vortex configurations were presented for the first time by Nielsen and Olesen [3], which showed that electrically neutral vortices in the Maxwell-Higgs model correspond to the Abrikosov ones. The existence of electrically charged vortex solutions was verified in both the Chern-Simons-Higgs (CSH) [4, 5] and Maxwell-Chern-Simons-Higgs (MCSH) [6] models. Vortices were also investigated in the $O(3)$ model framework supplemented with an Abelian gauge sector.

The nonlinear sigma $O(3)$ model in $(1+2)$ dimensions [7] has become popular in field theory due to some remarkable features and many possible applications to condensed matter physics [8]. One feature which has attracted considerable attention is the fact it provides topological stable solitonic solutions that are exactly integrable in Bogomol'nyi limit [9]. These solutions can be described as a map from a spherical surface that represents the two-dimensional physical space to a spherical surface in the internal field space, being classified according to the second homotopy group $\Pi_2(S_2) = \mathbb{Z}$. This model, however, presents a serious drawback: as the solutions are scale invariant they can undergo arbitrary size changing over time with no energy cost, preventing particle interpretation [10]. Some initial ways to circumvent this difficulty were proposed, involving the consideration of terms with a distinct number of derivative in relation to the sigma model Lagrangian [11], or the construction of Q-lumps by means of a particular potential in the $O(3)$ model [12]. Another interesting way to break the scale invariance consists of gauging the $U(1)$ subgroup and including a specific potential term in order to provide self-dual solutions. This task was initially

implemented by Schroers [13], with the dynamics of the gauge field being governed by a Maxwell term, and providing topological soliton solutions with arbitrary magnetic flux. The gauge dynamics can be also controlled by the Chern-Simons term [14], yielding topological and nontopological soliton solutions. In both cases topological solitons are infinitely degenerate in a given topological sector. Such a degenerescence can be lifted by choosing a self-interacting potential with a symmetry breaking minima [15, 16], which yields topological magnetic Bogomol'nyi-Prasad-Sommerfield (BPS) vortices. This potential introduces a new topology in which the infinite circle of physical space is mapped in the equatorial circle in the internal space so that the solitons are now classified by the first homotopy group $\Pi_1(S_1) = \mathbb{Z}$. Vortex configurations were also investigated in the context of a modified gauged $O(3)$ model in which the gauge field is nonminimally coupled to the σ field [17].

The study of topological defects in several different theoretical frameworks has been an issue of permanent interest in the recent years. Solitons and vortex configurations have been addressed in field models composed of generalizing dielectric functions with worthy new results [18]. Among these new investigations we can include there a search of topological defects in field models endowed with Lorentz symmetry breaking terms.

Lorentz symmetry violating field theories have been extensively investigated since 1996, mainly in the framework of the standard model extension [19, 20]. Such theoretical framework allows us to examine the effects of Lorentz violation in physical systems, also involving photon-fermion interactions [21], bumblebee models [22], fermion systems and radiative corrections [23], renormalization aspects [24], and the imposition of upper bounds on the magnitude of the Lorentz-violating (LV) coefficients [25–28]. LV theories are also connected to models containing higher-order derivative terms [29] and higher-dimension operators [30], and topological aspects of physical systems [31, 32].

The formation of defects in field model with LV term was considered in some situations, embracing solitons generated by scalar fields [33], Abelian monopoles [34], general defects engendered by tensor fields [35], oscillon

^{*}Electronic address: rodolfo.casana@gmail.com

[†]Electronic address: cfarias@gmail.com

[‡]Electronic address: manojr.ufma@gmail.com

configurations [36, 37]. Explicit BPS vortex solutions in Lorentz-violating scenarios were analyzed in Refs. [38–43].

Into the proposal of examining defects in new scenarios, this work aims at elucidating how the structure of topological defects in a gauged $O(3)$ nonlinear sigma model is modified by Lorentz violation. More specifically, we address the effects of introducing CPT -even and Lorentz-violating terms both in the Abelian gauge sector and the σ sector, as described in Sec. II. The particular case in which the solutions are purely magnetic is developed in Sec. III. In Sec. IV, the LV parameters are chosen to allow the existence of magnetic configurations also carrying an electric field but a null total electric charge. In both cases the BPS formalism is implemented, yielding self-dual equations for the scalar and gauge fields. Some limit cases on the LV parameters are discussed. We show that the energy and the magnetic flux of the vortex solutions are proportional to the winding number and depend explicitly on the LV parameters belonging to the σ sector. In Sec. V, we present our conclusions and perspectives.

II. THE LORENTZ-VIOLATING GAUGED $O(3)$ σ MODEL

The starting point is the $(1+2)$ -dimensional Lagrangian density describing the gauged $O(3)$ σ model studied in Ref. [16], enriched by CPT -even and Lorentz-violating terms,

$$\mathcal{L} = \frac{1}{2} \left(D^\mu \vec{\phi} \right) \cdot \left(D_\mu \vec{\phi} \right) + \frac{1}{2} (k_{\phi\phi})^{\mu\nu} \left(D_\mu \vec{\phi} \right) \cdot \left(D_\nu \vec{\phi} \right) - \frac{1}{4} F_{\mu\nu} F^{\mu\nu} - \frac{1}{2} \kappa^{\rho\alpha} F_{\rho\sigma} F_\alpha^\sigma - U, \quad (1)$$

where $\vec{\phi} = (\phi_1, \phi_2, \phi_3)$ is a triplet of real scalar fields constituting a vector in the internal space with fixed norm, $\vec{\phi} \cdot \vec{\phi} = 1$, which describes an $O(3)$ nonlinear σ model. Such a scalar sector is coupled to the Maxwell field, with $F_{\mu\nu} = \partial_\mu A_\nu - \partial_\nu A_\mu$ being the Maxwell tensor. The tensor $(k_{\phi\phi})^{\mu\nu}$ is real and symmetric containing the LV and CPT -even parameters in the σ sector, while $\kappa^{\rho\alpha}$ is a symmetric tensor which encloses CPT -even and LV coefficients in the electromagnetic sector [19, 26]. The potential U describes some convenient interaction producing BPS vortices.

The coupling between the gauge field and the triplet scalar field is given by the minimal covariant derivative

$$D_\mu \vec{\phi} = \partial_\mu \vec{\phi} - A_\mu \hat{n}_3 \times \vec{\phi}, \quad (2)$$

with \hat{n}_3 representing the 3-direction in the internal scalar field space. The equation of motion for the gauge field reads

$$\partial_\nu F^{\nu\mu} + \kappa^{\nu\alpha} \partial_\nu F_\alpha^\mu - \kappa^{\mu\alpha} \partial_\nu F_\alpha^\nu = j^\mu, \quad (3)$$

where

$$j^\mu = [g^{\mu\nu} + (k_{\phi\phi})^{\mu\nu}] \hat{n}_3 \cdot \left(\vec{\phi} \times D_\nu \vec{\phi} \right), \quad (4)$$

is the conserved current density that generalizes the one of Ref. [16], that is, $j^\mu = \hat{n}_3 \cdot \left(\vec{\phi} \times D_\nu \vec{\phi} \right)$. The equation of motion of the σ field is

$$[g^{\mu\nu} + (k_{\phi\phi})^{\mu\nu}] D_\mu D_\nu \vec{\phi} = \left(\vec{\phi} \cdot \frac{\partial U}{\partial \vec{\phi}} \right) \vec{\phi} - \frac{\partial U}{\partial \vec{\phi}} + [g^{\mu\nu} + (k_{\phi\phi})^{\mu\nu}] \left(\vec{\phi} \cdot D_\mu D_\nu \vec{\phi} \right) \vec{\phi}. \quad (5)$$

As we are interested in a solitonic solution in the static regime, we first write the static Gauss law

$$L_{ij} \partial_i \partial_j A_0 + \kappa_{0i} \epsilon_{ij} \partial_j B = (k_{\phi\phi})_{0i} \hat{n}_3 \cdot \left(\vec{\phi} \times D_i \vec{\phi} \right) + [1 + (k_{\phi\phi})_{00}] \left[(\phi_1)^2 + (\phi_2)^2 \right] A_0, \quad (6)$$

where we have introduced the symmetric matrix

$$L_{ij} = (1 + \kappa_{00}) \delta_{ij} - \kappa_{ij}. \quad (7)$$

With the finality to attain self-dual configurations, we have selected $(k_{\phi\phi})_{0i} = 0$. Such a choice allows us to study two cases. The first one consists in choosing $\kappa_{0i} = 0$, for which the Gauss law is

$$L_{ij} \partial_i \partial_j A_0 = [1 + (k_{\phi\phi})_{00}] \left[(\phi_1)^2 + (\phi_2)^2 \right] A_0. \quad (8)$$

Because the condition $A_0 = 0$ satisfies identically the Gauss law, this case describes purely magnetic solutions. The second case to consider is $\kappa_{0i} \neq 0$, this time the Gauss law becomes

$$L_{ij} \partial_i \partial_j A_0 + \kappa_{0i} \epsilon_{ij} \partial_j B = [1 + (k_{\phi\phi})_{00}] \left[(\phi_1)^2 + (\phi_2)^2 \right] A_0, \quad (9)$$

and the solutions also possess an electric field but the total electric charge is zero.

By considering the condition $(k_{\phi\phi})_{0i} = 0$, the static Ampère law reads

$$N_{ji} \partial_i B = -\kappa_{0i} \partial_i \partial_j A_0 + \kappa_{0j} \partial_i \partial_i A_0 + \left[\delta_{ji} - (k_{\phi\phi})_{ji} \right] \hat{n}_3 \cdot \left(\vec{\phi} \times D_i \vec{\phi} \right), \quad (10)$$

where we have defined the antisymmetric matrix

$$N_{ji} = \epsilon_{ji} - \epsilon_{jm} \kappa_{mi} - \kappa_{jm} \epsilon_{mi}. \quad (11)$$

In the following we study the two cases mentioned above. We first study the purely magnetic solutions, and in the sequel, the ones carrying a magnetic and an electric field.

III. PURELY MAGNETIC SELF-DUAL CONFIGURATIONS IN A CPT -EVEN AND LV GAUGED $O(3)$ σ MODEL

The purely magnetic solutions are obtained by considering the conditions $(k_{\phi\phi})_{0i} = 0$, $\kappa_{0i} = 0$, $A_0 = 0$, whose energy is

$$E = \int d^2x \left(\frac{1}{2} (1 - \kappa_{ii}) B^2 + \frac{1}{2} \tilde{D}_k \vec{\phi} \cdot \tilde{D}_k \vec{\phi} + U \right), \quad (12)$$

where $\kappa_{ii} = \kappa_{11} + \kappa_{22}$ and we have defined $\tilde{D}_k \vec{\phi}$ by

$$\tilde{D}_k \vec{\phi} = M_{kj} D_j \vec{\phi}, \quad (13)$$

$$\delta_{jk} - (k_{\phi\phi})_{jk} = M_{ij} M_{ik}, \quad (14)$$

where the coefficients M_{ij} define the matrix \mathbb{M} englobing the spatial LV coefficients of the σ sector. Before implementing the BPS formalism, we introduce the identity

$$\begin{aligned} \frac{1}{2} \tilde{D}_k \vec{\phi} \cdot \tilde{D}_k \vec{\phi} &= \frac{1}{4} \left(\tilde{D}_j \vec{\phi} \pm \epsilon_{jm} \vec{\phi} \times \tilde{D}_m \vec{\phi} \right)^2 \\ &\mp (\det \mathbb{M}) \phi_3 B \pm (\det \mathbb{M}) \epsilon_{ik} \partial_i (A_k \phi_3) \\ &\pm (\det \mathbb{M}) \vec{\phi} \cdot \left(\partial_1 \vec{\phi} \times \partial_2 \vec{\phi} \right), \end{aligned} \quad (15)$$

which allows us to express the energy (12) as

$$\begin{aligned} E &= \int d^2x \left\{ \frac{1}{4} \left(\tilde{D}_j \vec{\phi} \pm \epsilon_{jm} \vec{\phi} \times \tilde{D}_m \vec{\phi} \right)^2 \right. \\ &\quad \left. + \frac{1}{2} (1 - \kappa_{ii}) \left(B \mp \sqrt{\frac{2U}{1 - \kappa_{ii}}} \right)^2 \right. \\ &\quad \left. \pm (\det \mathbb{M}) \left[\vec{\phi} \cdot \left(\partial_1 \vec{\phi} \times \partial_2 \vec{\phi} \right) + \epsilon_{ik} \partial_i (A_k \phi_3) \right] \right. \\ &\quad \left. \pm B \left[\sqrt{2(1 - \kappa_{ii})U} - (\det \mathbb{M}) \phi_3 \right] \right\}. \end{aligned} \quad (16)$$

The integration of the expression in the third row of Eq. (16),

$$T_0 = \frac{(\det \mathbb{M})}{4\pi} \int d^2x \left[\vec{\phi} \cdot \left(\partial_1 \vec{\phi} \times \partial_2 \vec{\phi} \right) + \epsilon_{ik} \partial_i (A_k \phi_3) \right], \quad (17)$$

is the topological charge of the model, which depends on the Lorentz violation introduced in the σ sector - see the factor $\det \mathbb{M}$ and on the boundary conditions used to compute the integral. However, the integrand keeps the same form of the one of Ref. [16]. In Sec. III A, we explicitly compute the associated topological charge. We can also infer the existence of a conserved current,

$$K_\mu = \frac{(\det \mathbb{M})}{8\pi} \epsilon_{\mu\alpha\beta} \left[\vec{\phi} \cdot \left(D^\alpha \vec{\phi} \times D^\beta \vec{\phi} \right) + F^{\alpha\beta} \phi_3 \right], \quad (18)$$

whose component K_0 , whenever integrated over the space, yields the conserved topological charge (17).

The fourth row of Eq. (16) becomes null by choosing the potential,

$$U = \frac{(\det \mathbb{M})^2}{2(1 - \kappa_{ii})} \phi_3^2, \quad (19)$$

that is the one providing self-dual configurations. It corresponds to the functional form of the one of Ref. [16], $\phi_3^2/2$, multiplied by LV terms, and presents the same minimal configurations, that is,

$$\phi_3^2 = 0, \quad \phi_1^2 + \phi_2^2 = 1. \quad (20)$$

Thus, the energy (16) is written as

$$\begin{aligned} E &= \pm 4\pi T_0 \\ &+ \int d^2x \left\{ \frac{1}{4} \left(\tilde{D}_j \vec{\phi} \pm \epsilon_{jm} \vec{\phi} \times \tilde{D}_m \vec{\phi} \right)^2 \right. \\ &\quad \left. + \frac{1}{2} (1 - \kappa_{ii}) \left(B \mp \frac{\det \mathbb{M}}{1 - \kappa_{ii}} \phi_3 \right)^2 \right\}. \end{aligned} \quad (21)$$

We finally notice that the energy (21) has a lower bound

$$E \geq \pm 4\pi T_0, \quad (22)$$

which is attained when the field configurations satisfy the self-dual or BPS equations,

$$\tilde{D}_j \vec{\phi} \pm \epsilon_{jm} \vec{\phi} \times \tilde{D}_m \vec{\phi} = 0, \quad (23)$$

$$B = \pm \frac{\det \mathbb{M}}{1 - \kappa_{ii}} \phi_3. \quad (24)$$

Therefore, we have established the conditions that assure the existence of purely magnetic self-dual configurations in a *CPT*-even and Lorentz-violating $O(3)$ σ model. The sign \pm in Eq. (22) indicates that the topological charge T_0 can be positive or negative, once the energy is always positive.

For completeness, as happens in the Lorentz-invariant gauged model of Refs. [13, 16], it is possible to show the existence of an alternative form for the BPS equations (23) and (24) by stereographically projecting the target space S^2 into $C \cup \{\infty\}$. For it, we define the complex variable,

$$\omega = \frac{\phi_1 + i\phi_2}{(1 + \phi_3)}, \quad (25)$$

in terms of which the BPS equations are rewritten as

$$\tilde{\mathcal{D}}_1 \omega = \mp i \tilde{\mathcal{D}}_2 \omega, \quad (26)$$

$$F_{12} = \pm \frac{(\det \mathbb{M})}{(1 - \kappa_{ii})} \frac{(1 - |\omega|^2)}{(1 + |\omega|^2)}, \quad (27)$$

with $\tilde{\mathcal{D}}_k = M_{kj} (\partial_j - iA_j)$. By combining these equations, we obtain

$$\left[\delta_{jk} - (k_{\phi\phi})_{jk} \right] \partial_j \partial_k \ln |\omega| = \frac{(\det \mathbb{M})^2}{1 - \kappa_{ii}} \tanh \ln |\omega|, \quad (28)$$

remembering that the matrices $\delta_{jk} - (k_{\phi\phi})_{jk}$ and M_{jk} are related via Eq. (14). In the absence of Lorentz-violation, $M_{kj} = \delta_{kj}$, $\kappa_{ii} = 0$, and the BPS equations (26) and (27) easily recover the ones of Ref. [16], as expected.

Below we analyze a particular Ansatz describing the axially symmetric vortices.

A. Axially symmetrical purely magnetic self-dual solutions

For the energy to be finite, the field $\vec{\phi}$ should go to one of the minimum configurations of the potential, stated in Eq. (20). This is reached following a similar ansatz to the one introduced in Ref. [16] for axially symmetric vortices:

$$\begin{aligned}\phi_1 &= \sin g(r) \cos\left(\frac{n}{\Lambda}\theta\right), \quad \phi_2 = \sin g(r) \sin\left(\frac{n}{\Lambda}\theta\right), \\ \phi_3 &= \cos g(r), \quad A_\theta = -\frac{1}{r} \left[a(r) - \frac{n}{\Lambda}\right],\end{aligned}\quad (29)$$

with the radial functions, g , a , being well behaved and satisfying the boundary conditions,

$$g(0) = 0, \quad a(0) = \frac{n}{\Lambda}, \quad (30)$$

$$g(\infty) = \frac{\pi}{2}, \quad a(\infty) = 0, \quad (31)$$

which are compatible with the vacuum configurations of the potential when $r \rightarrow \infty$. Here, n is the winding number, a non-null integer, expressing the topological feature of the solutions. The boundary condition of the vector potential is now modified by the presence of the constant Λ , defined in terms of the Lorentz-violating parameters belonging to the σ sector,

$$\Lambda = \sqrt{\frac{1 - (k_{\phi\phi})_{\theta\theta}}{1 - (k_{\phi\phi})_{rr}}}. \quad (32)$$

It is worthwhile to clarify the reason for introducing the LV parameter Λ both in the ansatz (29) as in the boundary condition $a(0) = n/\Lambda$. Its presence guarantees that when $r \rightarrow 0$, the profile $g(r)$ is proportional to $r^{|n|}$ [see Eqs. (46) and (83)], as happens in the usual vortex solutions. We should also mention that the infinite circle (in coordinate space) is mapped on the equatorial circle in the internal space $\vec{\phi} = (\phi_1, \phi_2, 0)$, with $\phi_1^2 + \phi_2^2 = 1$. The associated topological solutions are not infinitely degenerated in each sector.

In the *ansatz* (29), the magnetic field B reads,

$$B(r) = -\frac{a'}{r}, \quad (33)$$

where $'$ stands for the radial derivative. In the same way, the BPS equations (23) and (24) read

$$g' = \pm \Lambda \frac{a}{r} \sin g, \quad (34)$$

$$B = -\frac{a'}{r} = \pm \frac{\eta}{1 - \kappa_{ii}} \cos g, \quad (35)$$

where η is

$$\eta = \det \mathbb{M} = \sqrt{[1 - (k_{\phi\phi})_{\theta\theta}][1 - (k_{\phi\phi})_{rr}]}. \quad (36)$$

The expression (36) could lead us to interpret the matrix \mathbb{M} as being a diagonal one, which is not correct. It becomes clearer by writing Eq. (14) in polar coordinates:

$$\begin{aligned}(k_{\phi\phi})_{rr} &= 1 - M_{rr}^2 - M_{\theta r}^2, \\ (k_{\phi\phi})_{r\theta} &= (k_{\phi\phi})_{\theta r} = -M_{rr}M_{r\theta} - M_{\theta\theta}M_{\theta r}, \\ (k_{\phi\phi})_{\theta\theta} &= 1 - M_{\theta\theta}^2 - M_{r\theta}^2.\end{aligned}\quad (37)$$

For the axially symmetric vortices, the condition $(k_{\phi\phi})_{r\theta} = 0$ is a requirement for the BPS equation (23) to engender Eq. (34). Consequently, the matrix $(k_{\phi\phi})$ becomes diagonal, but the same does not occur with \mathbb{M} . We should clarify that the fact of $(k_{\phi\phi})$ being diagonal in polar coordinates does not imply that it will also be in Cartesian coordinates.

Under the boundary conditions (30) and (31), the energy of the self-dual solutions is

$$E_{BPS} = \pm 2\pi \frac{\eta}{\Lambda} n, \quad (38)$$

which, besides being proportional to the winding number, also depends explicitly on the Lorentz violation factor η/Λ , belonging to the σ -sector. Here, positive (negative) sign is associated with positive (negative) values of n .

The BPS energy density, ε_{BPS} , which leads to the BPS energy $E_{BPS} = 2\pi \int dr r \varepsilon_{BPS}(r)$, is

$$\varepsilon_{BPS}(r) = (1 - \kappa_{ii}) B^2 + \Lambda \eta \left(\frac{a}{r} \sin g\right)^2. \quad (39)$$

It will be positive-definite whenever $\kappa_{ii} < 1$ and $\Lambda \eta > 0$.

By using the *Ansatz* (29) and the boundary conditions (30)-(31), we can compute the quantity T_0 in Eq. (17),

$$\begin{aligned}\int d^2x \vec{\phi} \cdot (\partial_1 \vec{\phi} \times \partial_2 \vec{\phi}) &= -2\pi \frac{n}{\Lambda} \int_0^\infty dr (\cos g)', \\ &= -2\pi \frac{n}{\Lambda} [\cos g(\infty) - \cos g(0)] = 2\pi \frac{n}{\Lambda},\end{aligned}\quad (40)$$

$$\int d^2x \epsilon_{ik} \partial_i (A_k \phi_3) = -2\pi \int_0^\infty dr \left[\left(a - \frac{n}{\Lambda}\right) \cos g\right]' = 0.$$

We thus show how the topological charge,

$$T_0 = \frac{\eta}{2} \frac{n}{\Lambda}, \quad (41)$$

is modified by the LV coefficients, recovering the usual charge, $T_0 = n/2$, in the absence of Lorentz violation.

It is important to point out that the boundary conditions (30) and (31) provide solutions $g(r)$ covering only the upper hemisphere of the internal space. For solutions $g(r)$ covering the lower hemisphere, we use the following boundary conditions:

$$g(0) = \pi, \quad a(0) = \frac{n}{\Lambda}, \quad (42)$$

$$g(\infty) = \frac{\pi}{2}, \quad a(\infty) = 0. \quad (43)$$

A rapid analysis allows us to infer that the solutions corresponding to the lower hemisphere can be obtained starting with the ones of the upper hemisphere by doing the following correspondence

$$g_{lower}(r) = \pi - g_{upper}(r), \quad (44)$$

$$a_{lower}(r) = -a_{upper}(r), \quad (45)$$

where $g_{upper}(r)$ and $a_{upper}(r)$ are solutions of the upper hemisphere for positive (negative) n and, $g_{lower}(r)$ and $a_{lower}(r)$ are solutions of the lower hemisphere corresponding exactly to negative (positive) n . Consequently, for a given n the solutions in the upper and lower hemispheres have opposite topological charges.

1. Checking the behavior at boundaries

By solving the BPS equations (34) and (35) near the origin, one attains

$$g(r) \approx G_n r^n + \dots, \quad (46)$$

$$a(r) \approx \frac{n}{\Lambda} - \frac{\eta}{2(1 - \kappa_{ii})} r^2 + \dots, \quad (47)$$

where G_n is unique for a fixed n and it is numerically computed. This behavior is compatible with the boundary conditions (30).

By solving the BPS equations (34) and (35) for $r \rightarrow \infty$, the asymptotic behavior is

$$g(r) \approx \frac{\pi}{2} - C_\infty \frac{e^{-mr}}{\sqrt{r}} + \dots, \quad (48)$$

$$a(r) \approx \frac{mC_\infty}{\Lambda} \sqrt{r} e^{-mr} + \dots, \quad (49)$$

with C_∞ being a numerically determined constant. Such behavior is supported by the boundary conditions (31). The constant m is the mass of the self-dual bosons, given by

$$m = \sqrt{\frac{\eta\Lambda}{(1 - \kappa_{ii})}}. \quad (50)$$

In the absence of Lorentz violation, the mass of the self-dual bosons is equal to 1. Considering LV corrections, the mass (50) can be larger or smaller than 1, which corresponds to a narrower or wider vortex core, respectively.

B. Numerical analysis of the Lorentz-violating purely magnetic self-dual vortices

We first write the self-dual equations of the gauged $O(3)$ σ model in absence of Lorentz violation. These BPS equations can be directly obtained from Eqs. (34)

and (35) by setting $\Lambda = 1$, $\eta = 1$, and $\kappa_{ii} = 0$, which reads

$$g' = \pm \frac{a}{r} \sin g, \quad (51)$$

$$B = -\frac{a'}{r} = \pm \cos g. \quad (52)$$

By comparing Eqs. (35) and (52) it is easy to notice that Lorentz violation can provide larger or smaller values for the magnetic field amplitude at the origin. More detailed analysis of the Lorentz-violating BPS solutions is performed by numerically solving the differential equations (34) and (35). In particular, we comment on the main aspects in which such solutions differ from the ones obtained in the absence of Lorentz violation, described by Eqs. (51) and (52).

The BPS equations (34) and (35) provide a large family of self-dual solutions, each one depending on the values of the Lorentz-violating parameters. Among these many possibilities, we present the solutions for $n = 1$, $\kappa_{ii} = 0.1$, $\eta = 0.9999\Lambda$, and the following values for Λ :

$$\Lambda_1 = 0.5, \Lambda_2 = 0.75, \Lambda_3 = 1, \quad (53)$$

$$\Lambda_4 = 1.25, \Lambda_5 = 1.5, \Lambda_6 = 1.75. \quad (54)$$

Such values of the Lorentz-violating parameters provide the following masses for the self-dual bosons:

$$m_1 = 0.52702, m_2 = 0.79053, m_3 = 1.05404, \quad (55)$$

$$m_4 = 1.31755, m_5 = 1.58106, m_6 = 1.84457, \quad (56)$$

computed via Eq. (50), respectively.

Figures 1–4 present some profiles (for the winding number $n = 1$) for the σ field, gauge field, magnetic field, and BPS energy density of the purely magnetic self-dual solutions. The black solid line represents the BPS profiles in the absence of Lorentz violations. The green lines represent the solutions with $\Lambda < 1$ (or equivalently $m < 1$), while the red lines depict the ones with $\Lambda \geq 1$ (or equivalently $m \geq 1$).

Figure 1 depicts the numerical results obtained for the profiles of the σ field, showing that they turn out to be around the ones of the model in the absence of Lorentz violation. These profiles become wider for $\Lambda < 1$, otherwise, for $\Lambda \geq 1$, the profiles become progressively narrower for increasing values of Λ , as expected.

Figure 2 displays the profiles of the vector potential. As happens with the σ -field profiles, they become wider for decreasing values of $\Lambda < 1$ and narrower for increasing values of $\Lambda \geq 1$. The novelty is the dependence of $a(0)$ in terms of Λ^{-1} , which is compatible with the boundary conditions imposed in Eq. (30).

Figure 3 depicts the magnetic field profiles. They are lumps centered at the origin whose amplitudes are proportional to $\eta(1 - \kappa_{ii})^{-1}$. The LV parameters were fixed as $\kappa_{ii} = 0.1$, $\eta = 0.9999\Lambda$, then for increasing values of Λ

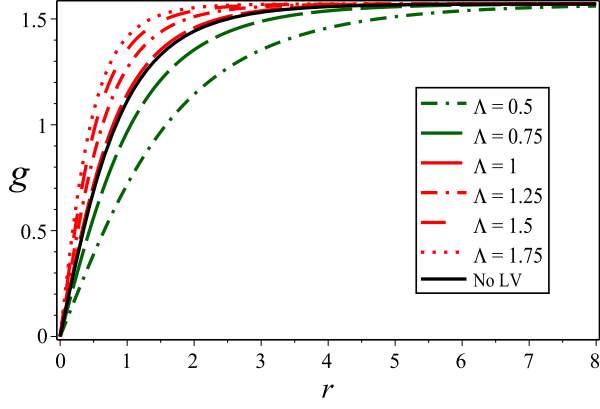


FIG. 1: The profiles of the σ field, $g(r)$, for winding number $n = 1$. The black line is the profile in the absence of Lorentz violation. The green lines depict the profiles of the self-dual solutions with masses $m < 1$. The red lines represent self-dual solutions with masses $m > 1$.

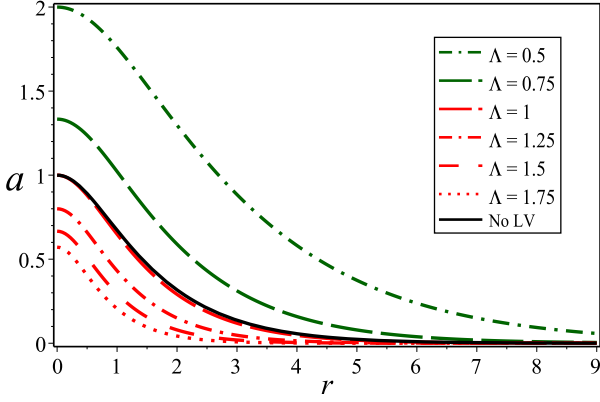


FIG. 2: The profiles of the gauge field $a(r)$.

(red lines), amplitudes higher than 1 (black line, the amplitude in the absence of Lorentz violation) and narrower profiles are obtained, otherwise, amplitudes smaller than 1 and wider profiles are revealed for decreasing values of Λ (green lines).

The profiles of the BPS energy density are shown in Fig. 4, which also are lumps centered at origin like the ones of the magnetic field. Their amplitudes at origin are given by $1.1109\Lambda^2 + 0.9999(G_1)^2$, where G_1 is defined in (46). Numerically, it is shown that G_1 grows or diminishes with Λ , following its behavior.

We remark that Lorentz violation works as a factor able to reduce or increment the radial extension of the vortex core, the amplitude of the magnetic field, and BPS energy density, keeping the topological character and enriching the diversity of purely magnetic self-dual solutions of the gauged $O(3)$ σ model.

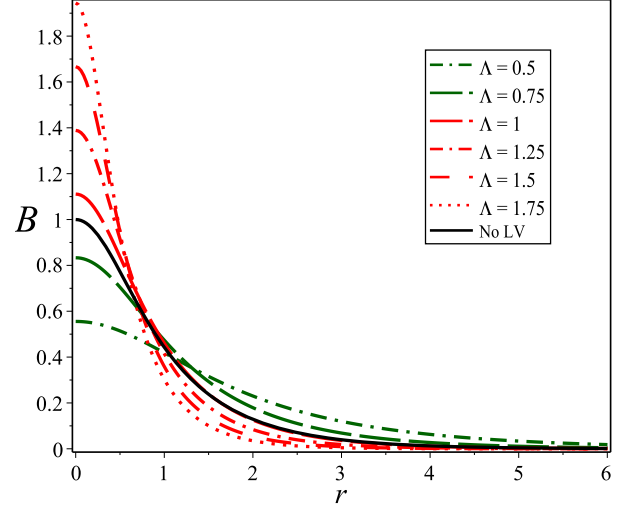


FIG. 3: The profiles of the magnetic field $B(r)$.

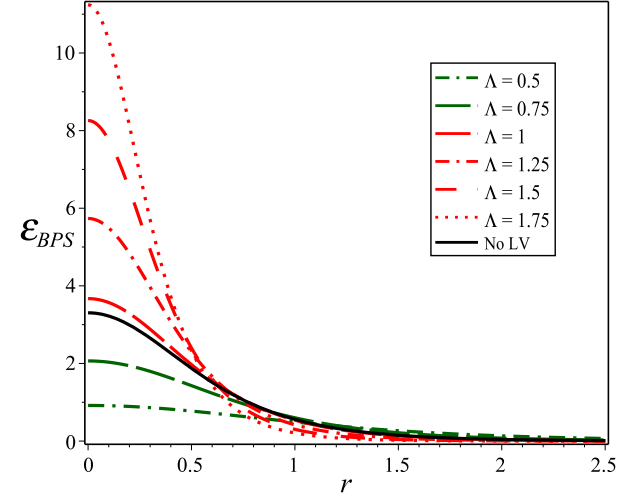


FIG. 4: The profiles of the BPS energy density field $\epsilon_{BPS}(r)$.

IV. MAGNETIC SELF-DUAL CONFIGURATIONS CARRYING AN ELECTRIC FIELD IN A CPT -EVEN AND LV GAUGED $O(3)$ σ MODEL

In this section, we describe the configurations possessing an electric field but a null total electric charge, associated with the conditions $(k_{\phi\phi})_{0i} = 0$, $\kappa_{0i} \neq 0$, and the Gauss law (9). In order to provide a correct description of magnetic self-dual configurations carrying an electric field, we must modify the Lagrangian density (1) by in-

roducing a neutral scalar field Ψ ,

$$\begin{aligned} \mathcal{L} = & -\frac{1}{4}F^{\mu\nu}F_{\mu\nu} - \frac{1}{2}\kappa_{\nu\rho}F^{\mu\nu}F_{\mu}{}^{\rho} \\ & + \frac{1}{2}\left(D^{\mu}\vec{\phi}\right) \cdot \left(D_{\mu}\vec{\phi}\right) + \frac{1}{2}(k_{\phi\phi})^{\mu\nu}\left(D_{\mu}\vec{\phi}\right) \cdot \left(D_{\nu}\vec{\phi}\right) \\ & + \frac{1}{2}(1 + \kappa_{00})\partial_{\mu}\Psi\partial^{\mu}\Psi + \frac{1}{2}\kappa^{\mu\nu}\partial_{\mu}\Psi\partial_{\nu}\Psi \\ & - \frac{1}{2}\left[1 + (k_{\phi\phi})_{00}\right]\left[(\phi_1)^2 + (\phi_2)^2\right]\Psi^2 - U(\phi_3, \Psi), \end{aligned} \quad (57)$$

with the kinetic term of this new field also affected by the Lorentz-violating tensor $\kappa^{\mu\nu}$. The introduction of a neutral scalar field has the aim at providing a consistent description of the self-dual configurations carrying an electric field in our model. A similar situation was reported in the context of Maxwell-Chern-Simons gauged $O(3)$ sigma model [44]. The introduction of a neutral scalar field is a well established procedure for a consistent description of self-dual configurations and it was first reported [6] in Maxwell-Chern-Simons-Higgs models based in supersymmetric arguments. It was also successfully implemented in other subsequent extensions [45], including Lorentz-violating Maxwell-Higgs models [39, 43]. Furthermore, the introduction of the neutral field is a physical requirement for the existence of a $N = 2$ extended supersymmetric version of the model which supports charged solutions [17, 46]. As was shown by Witten and Olive [47], the central charge of the extended supersymmetric algebra is related to a topological quantum number which is related to the existence of a Bogomol'nyi bound and vice-versa.

The energy of the static solutions carrying an electric field is

$$\begin{aligned} E = & \int d^2x \left\{ \frac{1}{2}\tilde{D}_k\vec{\phi} \cdot \tilde{D}_k\vec{\phi} + \frac{1}{2}(1 - \kappa_{ii})B^2 + U \right. \\ & + \frac{1}{2}L_{ij}(\partial_i A_0)(\partial_j A_0) + \frac{1}{2}L_{ij}(\partial_i \Psi)(\partial_j \Psi) \\ & \left. + \frac{1}{2}[1 + (k_{\phi\phi})_{00}][(\phi_1)^2 + (\phi_2)^2][(A_0)^2 + \Psi^2] \right\}. \end{aligned} \quad (58)$$

By using the identity (15) and implementing the BPS

formalism, the energy becomes

$$\begin{aligned} E = & \int d^2x \left\{ \frac{1}{4}\left(\tilde{D}_j\vec{\phi} \pm \epsilon_{jm}\vec{\phi} \times \tilde{D}_m\vec{\phi}\right)^2 \right. \\ & + \frac{1}{2}(1 - \kappa_{ii})\left(B \mp \sqrt{\frac{2U}{1 - \kappa_{ii}}}\right)^2 \\ & + \frac{1}{2}L_{ij}(\partial_i A_0 \pm \partial_i \Psi)(\partial_j A_0 \pm \partial_j \Psi) \\ & + \frac{1}{2}[1 + (k_{\phi\phi})_{00}][(\phi_1)^2 + (\phi_2)^2][A_0 \pm \Psi]^2 \\ & \pm (\det \mathbb{M})\left[\vec{\phi} \cdot \left(\partial_1\vec{\phi} \times \partial_2\vec{\phi}\right) + \epsilon_{ik}\partial_i(A_k\phi_3)\right] \\ & \pm B\left[\sqrt{2(1 - \kappa_{ii})U} - (\det \mathbb{M})\phi_3\right] \\ & \mp L_{ij}(\partial_i A_0)(\partial_j \Psi) \\ & \left. \mp [1 + (k_{\phi\phi})_{00}][(\phi_1)^2 + (\phi_2)^2]A_0\Psi\right\}. \end{aligned} \quad (59)$$

With the Gauss law (9), the last term can be written as

$$L_{ij}\Psi\partial_i\partial_j A_0 + \kappa_{0i}\epsilon_{ij}\partial_j(\Psi B) - \kappa_{0i}\epsilon_{ij}B\partial_j\Psi, \quad (60)$$

which allows us to express the energy (59) as

$$\begin{aligned} E = & \int d^2x \left\{ \frac{1}{4}\left(\tilde{D}_j\vec{\phi} \pm \epsilon_{jm}\vec{\phi} \times \tilde{D}_m\vec{\phi}\right)^2 \right. \\ & + \frac{1}{2}(1 - \kappa_{ii})\left(B \mp \sqrt{\frac{2U}{1 - \kappa_{ii}}}\right)^2 \\ & + \frac{1}{2}L_{ij}(\partial_i A_0 \pm \partial_i \Psi)(\partial_j A_0 \pm \partial_j \Psi) \\ & + \frac{1}{2}[1 + (k_{\phi\phi})_{00}][(\phi_1)^2 + (\phi_2)^2][A_0 \pm \Psi]^2 \\ & \pm B\left[\sqrt{2(1 - \kappa_{ii})U} - (\det \mathbb{M})\phi_3 + \kappa_{0i}\epsilon_{ij}\partial_j\Psi\right] \\ & \pm (\det \mathbb{M})\left[\vec{\phi} \cdot \left(\partial_1\vec{\phi} \times \partial_2\vec{\phi}\right) + \epsilon_{jk}\partial_j(A_k\phi_3)\right] \\ & \left. \mp L_{ij}\partial_j(\Psi\partial_i A_0) \mp \kappa_{0i}\epsilon_{ij}\partial_j(\Psi B)\right\}. \end{aligned} \quad (61)$$

By requesting that the fifth row be null, we find the interaction potential U ,

$$U = \frac{1}{2(1 - \kappa_{ii})}[(\det \mathbb{M})\phi_3 - \kappa_{0i}\epsilon_{ij}\partial_j\Psi]^2, \quad (62)$$

which involves the presence of derivative terms and is the correct one for generating self-dual configurations. Potentials composed of derivative terms have also been observed in other Lorentz-violating Maxwell-Higgs models [39, 43]. Note that this potential is much more involved than the one in Ref. [16].

As happens in the purely magnetic case, the sixth row in Eq. (61) provides the topological charge of the model; see Eq. (17). By considering the fields going to zero at infinity, the integration of the terms in the seventh row

gives a null contribution to the energy. Thus, the energy of the solutions carrying an electric field becomes

$$\begin{aligned}
E = & \pm 4\pi T_0 \\
& + \int d^2x \left\{ \frac{1}{4} \left(\tilde{D}_j \vec{\phi} \pm \epsilon_{jm} \vec{\phi} \times \tilde{D}_m \vec{\phi} \right)^2 \right. \\
& + \frac{1}{2} (1 - \kappa_{ii}) \left(B \mp \frac{(\det \mathbb{M}) \phi_3 - \kappa_{0i} \epsilon_{ij} \partial_j \Psi}{1 - \kappa_{ii}} \right)^2 \\
& + \frac{1}{2} L_{ij} (\partial_i A_0 \pm \partial_i \Psi) (\partial_j A_0 \pm \partial_j \Psi) \\
& \left. + \frac{1}{2} [1 + (k_{\phi\phi})_{00}] [(\phi_1)^2 + (\phi_2)^2] [A_0 \pm \Psi]^2 \right\}.
\end{aligned} \tag{63}$$

Then, from Eq. (63) we see that energy is bounded from below,

$$E \geq \pm 4\pi T_0. \tag{64}$$

This lower bound is attained with the fields satisfying the self-dual or BPS equations,

$$\tilde{D}_j \vec{\phi} \pm \epsilon_{jm} \vec{\phi} \times \tilde{D}_m \vec{\phi} = 0, \tag{65}$$

$$B = \pm \frac{(\det \mathbb{M}) \phi_3 - \kappa_{0i} \epsilon_{ij} \partial_j \Psi}{1 - \kappa_{ii}}, \tag{66}$$

$$\partial_i A_0 \pm \partial_i \Psi = 0, \tag{67}$$

$$A_0 \pm \Psi = 0. \tag{68}$$

The condition $\Psi = \mp A_0$ saturates the two last equations. This way, the solitonic solutions also carrying an electric field are described by the BPS equations

$$\tilde{D}_j \vec{\phi} \pm \epsilon_{jm} \vec{\phi} \times \tilde{D}_m \vec{\phi} = 0, \tag{69}$$

$$B = \pm \frac{(\det \mathbb{M}) \phi_3}{1 - \kappa_{ii}} + \frac{\kappa_{0i} \epsilon_{ij} \partial_j A_0}{1 - \kappa_{ii}}, \tag{70}$$

and the Gauss law

$$L_{ij} \partial_i \partial_j A_0 + \kappa_{0i} \epsilon_{ij} \partial_j B = [1 + (k_{\phi\phi})_{00}] [(\phi_1)^2 + (\phi_2)^2] A_0. \tag{71}$$

Below we study the particular case of self-dual configurations, the axially symmetric vortices.

A. Axially symmetrical self-dual vortices carrying an electric field

By considering the axially symmetrical *ansatz* (29) and

$$A_0 = A_0(r), \tag{72}$$

the projected BPS equations (69) and (70) are written as

$$g' = \pm \Lambda \frac{a}{r} \sin g, \tag{73}$$

$$B = -\frac{a'}{r} = \pm \frac{\eta \cos g}{1 - \kappa_{ii}} - \frac{\kappa_{0\theta} A'_0}{1 - \kappa_{ii}}, \tag{74}$$

whereas the Gauss law (71) reads

$$(1 + \lambda_r) \frac{(r A'_0)'}{r} - \kappa_{0\theta} \frac{(r B)'}{r} = \eta \Lambda \Delta A_0 \sin^2 g. \tag{75}$$

Here, we have introduced

$$\lambda_r = \kappa_{00} - \kappa_{rr}, \tag{76}$$

$$\Delta = \frac{1 + (k_{\phi\phi})_{00}}{\eta \Lambda}, \tag{77}$$

and the constants Λ and η are defined in Eqs. (32) and (36), respectively.

The functions $g(r)$, $a(r)$ fulfill the same boundary conditions introduced in Eqs. (30) and (31) and the function $A_0(r)$ satisfies the boundary conditions (86)-(93), as will be shown explicitly in the manuscript.

Although presenting an electric field, the self-dual configurations described by Eqs. (73)-(75) possess a null total electric charge. This can be demonstrated easily by using the Gauss law (75) where the right-hand side defines the electric charge density $\rho = A_0 \sin^2 g$, whose integration provides the total electric charge of the self-dual configuration,

$$Q = 2\pi \int_0^\infty r \rho(r) dr. \tag{78}$$

By using the boundary conditions described in the previous paragraph, the integration of the Gauss law provides a null electric charge, that is,

$$Q = 0. \tag{79}$$

The BPS energy density is given by

$$\begin{aligned}
\varepsilon_{BPS}(r) = & (1 - \kappa_{ii}) B^2 + \eta \Lambda \left(\frac{a \sin g}{r} \right)^2 \\
& + \eta \Lambda \Delta (A_0 \sin g)^2 + (1 + \lambda_r) (A'_0)^2,
\end{aligned} \tag{80}$$

and is defined positive providing that

$$\kappa_{ii} < 1, \Delta > 0, \lambda_r > -1. \tag{81}$$

As in the purely magnetic case, the solutions $g(r)$ obtained from Eqs. (73)-(75) fulfilling the boundary conditions (30), (31), (86), (93) only cover the upper hemisphere of the internal space. The solutions $g(r)$ covering the lower hemisphere are obtained by solving the Eqs. (73)-(75) with the boundary conditions (42) and (43). Consequently, the solutions can be obtained starting from the first ones making the correspondence (44) and (45) and

$$(A_0)_{lower}(r) = -(A_0)_{upper}(r), \tag{82}$$

where $(A_0)_{upper}(r)$ represents solutions of the upper hemisphere for positive (negative) n and $(A_0)_{lower}(r)$

provides solutions of the lower hemisphere corresponding to negative (positive) n , respectively. Consequently, as happens in the purely magnetic case, for a given n the solutions obtained for the upper and lower hemispheres have opposite topological charge.

B. Behavior of the profiles at boundaries

By solving Eqs. (73)-(75) near to the origin, we obtain

$$g(r) \approx G_n r^n + \dots, \quad (83)$$

$$a(r) \approx \frac{n}{\Lambda} - \frac{1}{2} \frac{\eta(1+\lambda_r)}{\kappa_{0\theta}^2 + (1-\kappa_{ii})(1+\lambda_r)} r^2 + \dots, \quad (84)$$

$$A_0(r) \approx A_0(0) + \frac{\eta\kappa_{0\theta}}{\kappa_{0\theta}^2 + (1-\kappa_{ii})(1+\lambda_r)} r + \dots, \quad (85)$$

where $A_0(0)$ is determined numerically for every n . The last equation allows to set explicitly the boundary condition for A_0 at the origin

$$A'_0(0) = \frac{\eta\kappa_{0\theta}}{\kappa_{0\theta}^2 + (1-\kappa_{ii})(1+\lambda_r)}. \quad (86)$$

By solving the BPS equations when $r \rightarrow \infty$, we attain

$$g(r) \approx \frac{\pi}{2} - C_\infty \frac{e^{-mr}}{\sqrt{r}} + \dots, \quad (87)$$

$$a(r) \approx \frac{mC_\infty}{\Lambda} \sqrt{r} e^{-mr} + \dots, \quad (88)$$

$$A_0(r) \approx \frac{(1-\kappa_{ii})m^2 - \eta\Lambda}{\Lambda\kappa_{0\theta}m} C_\infty \frac{e^{-mr}}{\sqrt{r}} + \dots, \quad (89)$$

where C_∞ is a positive constant numerically determined. The mass of the self-dual bosons, m , is given by

$$m = \sqrt{\frac{\eta\Lambda(\beta_1 \pm \beta_2)}{2[\kappa_{0\theta}^2 + (1-\kappa_{ii})(1+\lambda_r)]}}, \quad (90)$$

with β_1 and β_2 being positive real numbers given by

$$\beta_1 = (1+\lambda_r) + \Delta(1-\kappa_{ii}), \quad (91)$$

$$\beta_2 = \sqrt{[(1+\lambda_r) - \Delta(1-\kappa_{ii})]^2 - 4\Delta\kappa_{0\theta}^2}. \quad (92)$$

For β_2 , the condition $[(1+\lambda_r) - \Delta(1-\kappa_{ii})]^2 \geq 4\Delta\kappa_{0\theta}^2$, must be satisfied. The signs in Eq. (90) will be used as follows: $+$ ($-$) for $(1+\lambda_r) - \Delta(1-\kappa_{ii}) > 0$ (< 0).

From Eq. (89), we obtain the boundary condition for $A_0(r)$ when $r \rightarrow \infty$,

$$A_0(\infty) = 0. \quad (93)$$

To finish, we present some limited cases on the LV parameters. When $\kappa_{0\theta} = 0$, Eq. (90) recovers the mass scale of uncharged BPS vortices:

$$m = \sqrt{\frac{\eta\Lambda}{1-\kappa_{ii}}}. \quad (94)$$

On the other hand, when $\beta_2 = 0$, the parity-odd coefficient can be expressed in terms of parity-even ones,

$$\kappa_{0\theta} = \pm \frac{|1+\lambda_r - \Delta(1-\kappa_{ii})|}{2\sqrt{\Delta}}, \quad (95)$$

and the mass scale becomes

$$m = \sqrt{\frac{2\eta\Lambda\Delta}{(1+\lambda_r) + \Delta(1-\kappa_{ii})}}. \quad (96)$$

Another interesting possibility is to set $\kappa_{ii} = 0$ and $\lambda_r = 0$ in Eq.(90), i.e., we can consider null the LV parity-even electromagnetic coefficients, getting

$$m = (\eta\Lambda)^{1/2} \sqrt{\frac{1+\Delta \pm \sqrt{(1-\Delta)^2 - 4\Delta\kappa_{0\theta}^2}}{2(1+\kappa_{0\theta}^2)}}, \quad (97)$$

with signal $+$ ($-$) for $1-\Delta > 0$ (< 0). This situation also provides Abrikosov-Nielsen-Olesen-like vortices whenever the condition,

$$(1-\Delta)^2 \geq 4\Delta\kappa_{0\theta}^2, \quad (98)$$

is satisfied. We remark that in the absence of LV in σ sector ($\Delta = \eta = \Lambda = 1$) it is impossible to obtain Abrikosov-Nielsen-Olesen-like vortices when κ_{ii} and λ_r are null because the mass scale (97) becomes a complex number.

C. Numerical analysis: A “charged” vortex configuration

We consider the case $\beta_2 = 0$, with $\kappa_{ii} = 0$, $\lambda_r = 0$. Then

$$\kappa_{0\theta} = \frac{\Delta-1}{2\sqrt{\Delta}}, \quad \Delta > 0. \quad (99)$$

In this way, the boundary conditions read

$$\begin{aligned} g(0) &= 0, \quad a(0) = n, \quad A'_0(0) = \frac{2\eta(\Delta-1)\sqrt{\Delta}}{(1+\Delta)^2}, \\ g(\infty) &= \frac{\pi}{2}, \quad a(\infty) = 0, \quad A_0(\infty) = 0. \end{aligned} \quad (100)$$

Hereafter, we consider $\Lambda = 1$ and $\eta = 1.05$. As a consequence the mass scale m is given by

$$m = \sqrt{\frac{2.1\Delta}{1+\Delta}}, \quad (101)$$

taking the values, $0 < m \leq \sqrt{2.1}$. We note that for $\Delta \ll 1$, the defect reaches its asymptotic values slowly. But when $\Delta \rightarrow 10/11$, the behavior is close to the profiles in the absence of Lorentz violation, because $m \rightarrow 1$ (see the solid black lines in Figs. 5-9). On the other hand,

for $\Delta \rightarrow \infty$, the mass scale reaches its maximum value $m \rightarrow \sqrt{2.1}$ (see the solid blue lines in Figs. 5-9).

We have depicted the profiles obtained from numerical solutions of Eqs. (73)-(75) under the boundary conditions (100). Without loss of generality, we have considered $n = 1$, with the solutions being compared with the profiles of the model in the absence of Lorentz violation (the solid black lines).

Figures 5 and 6 show the profiles of the σ field and the gauge field, respectively. For $\Delta \ll 1$, they are very spread and reach their asymptotic value slowly. When $\Delta \rightarrow 1$, they are narrower and attain the vacuum state more rapidly. For $0 < \Delta \leq 0.5$, the profiles are limited by the one in the absence of Lorentz violation ($\Delta = 1$, solid black line). However, for $\Delta \geq 2$, the profiles become wider but are limited by the width of the profile corresponding to $\Delta \rightarrow \infty$ (solid blue line). Numerical analysis showed that the profiles of the σ field and the gauge field in the interval $0.5 < \Delta < 2$ are almost overlapped with the ones obtained in the absence of Lorentz violation, which does not occur with the magnetic field and the BPS energy density.

The magnetic field behavior is shown in Fig. 7. For the range $0 < \Delta \leq 0.642$ (green lines), the profiles are lumps whose amplitudes at the origin increases whenever Δ augments, reaching the value $B(0) = 1$ for $\Delta = 0.642$. For $0.642 < \Delta < 5$, the profiles are also lumps centered at the origin. For $0.642 < \Delta < 1$ the amplitude increases attaining its maximum value $B(0) = 1.05$ when $\Delta = 1$; on the other hand, for $\Delta > 1$ the profile amplitude decreases while Δ increases continuously. For $5 < \Delta < 9$, the lumps present a deformation close to the origin. An interesting fact is observed when $\Delta > 9$: the deformed lump begins to become a ringlike profile. This way, for large values of Δ , the magnetic field approaches the CSH and MCSH ringlike profiles. This is an interesting effect produced by the mixing of the parity-odd ($\kappa_{0\theta}$) gauge LV coefficient and the parity-even (Δ) LV coefficient belonging to the σ sector. Such a behavior of the amplitude of the magnetic field at the origin can be verified by analyzing $B(0)$, which can be obtained directly from Eq. (84):

$$B(0) = \frac{4\eta\Delta}{(\Delta + 1)^2}, \quad (102)$$

which behaves as Δ^{-1} for large values of Δ , implying that the magnetic field at the origin goes to zero when $\Delta \rightarrow \infty$. This result is valid for all values of winding number n .

Another remarkable feature of this model is the localized magnetic field inversion. It takes place for $0 \leq \Delta < 0.7$, as is shown in Fig. 8, where a zoom was performed on the profiles with $0.01 \leq \Delta \leq 0.7$. One can clearly observe the localized magnetic field inversion, which is more pronounced for values of $\Delta < 0.6$. Around the value $\Delta \simeq 0.6$ the inversion becomes negligible, ceasing for larger values of Δ .

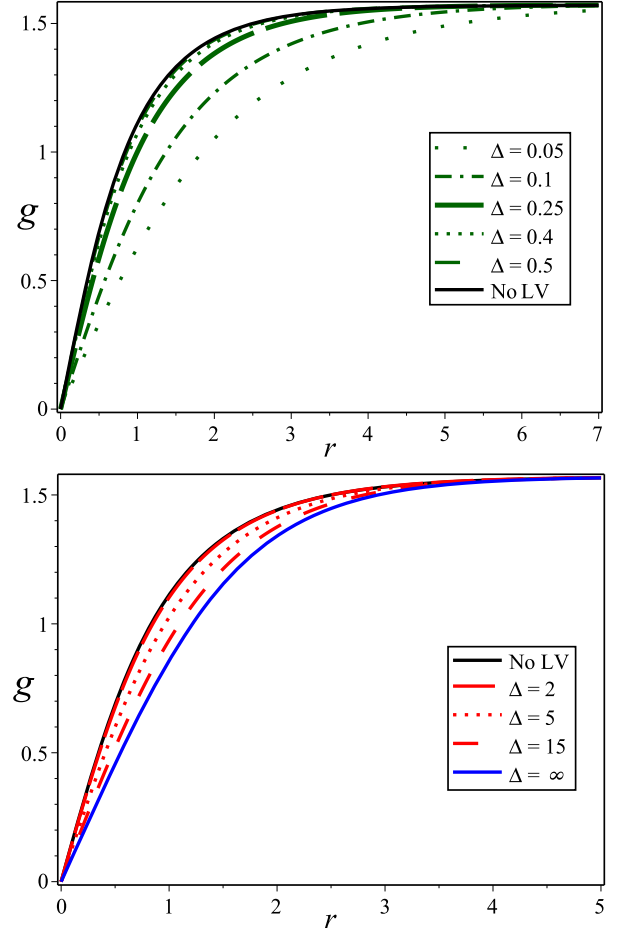


FIG. 5: The profiles of the σ field, $g(r)$, for winding number $n = 1$. The upper figure represents the profiles for $0 < \Delta \leq 0.5$ and the lower figure represents the profiles for $\Delta \geq 2$. The solid black line represents the profiles in absence of Lorentz violation. The blue line is the profile for $\Delta \rightarrow \infty$.

The magnetic field inversion is a relevant feature of this model and can be confirmed by means of an analytical analysis in the which one discusses the behavior of the magnetic field for sufficiently large values of r (i.e., $r \rightarrow \infty$). Here, we analyze the case of positive winding number. By considering $g(r) \rightarrow \pi/2$ when $r \rightarrow \infty$, the BPS equation (74) is simplified as

$$B(r) \simeq -\frac{\kappa_{0\theta}}{1 - \kappa_{ii}} A'_0(r). \quad (103)$$

The function $A'_0(r)$ can be easily computed from Eq. (89),

$$A'_0(r) \approx -\frac{(1 - \kappa_{ii})m^2 - \eta\Lambda}{\Lambda\kappa_{0\theta}m} C_\infty \left(m + \frac{1}{2r} \right) \frac{e^{-mr}}{\sqrt{r}} + \dots, \quad (104)$$

so that, for large values of r , the magnetic field behaves

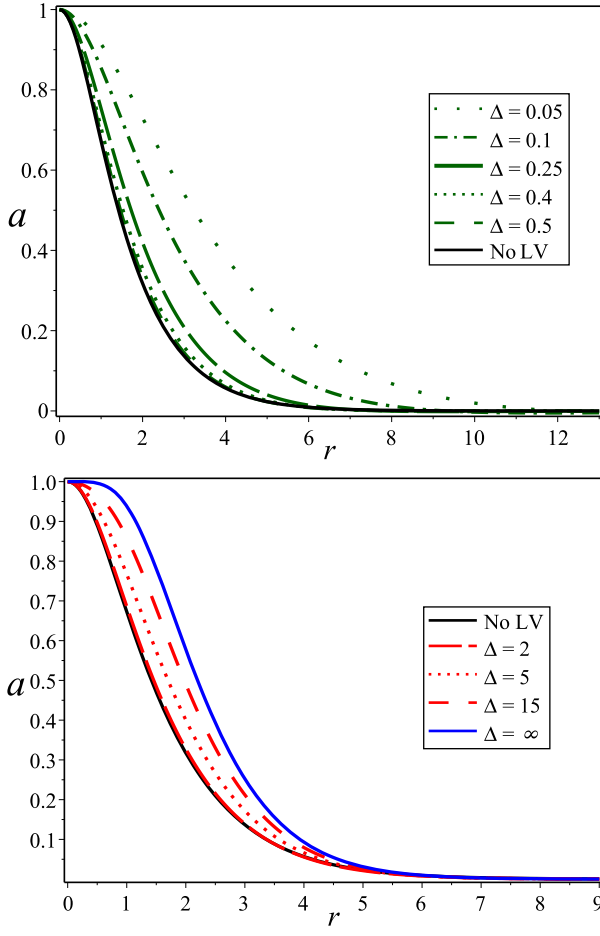


FIG. 6: The profiles of the gauge field, $a(r)$, for winding number $n = 1$. The legends are the same as in Fig. 5.

as

$$B(r) \simeq \frac{(1 - \kappa_{ii}) m^2 - \eta \Lambda}{(1 - \kappa_{ii}) \Lambda m} C_\infty \left(m + \frac{1}{2r} \right) \frac{e^{-mr}}{\sqrt{r}} + \dots \quad (105)$$

The only quantity that could be negative is $(1 - \kappa_{ii}) m^2 - \eta \Lambda$. Our case, with m given by (96), yields

$$\Delta(1 - \kappa_{ii}) < (1 + \lambda_r), \quad (106)$$

which, under the conditions $\kappa_{ii} = 0 = \lambda_r$ used in our numerical analysis, provides a negative magnetic field for large values of r when $\Delta < 1$. This fact, associated with a positive $B(0)$, indicates magnetic field inversion. This result is in complete agreement with the profiles depicted in Fig. 8. For $n < 0$, the reciprocal situation happens.

The magnetic field flipping finds applications in fractional vortices occurring in superconductors described by the two-component Ginzburg-Landau model [48].

Figure 9 presents the profiles for the BPS energy density, which are very similar to the ones of the magnetic field. For $0 < \Delta \lesssim 10$, they are lumps centered at the origin whose amplitude increases when Δ falls in the range $0 < \Delta \leq 1$, attaining its maximum value for $\Delta = 1$. For

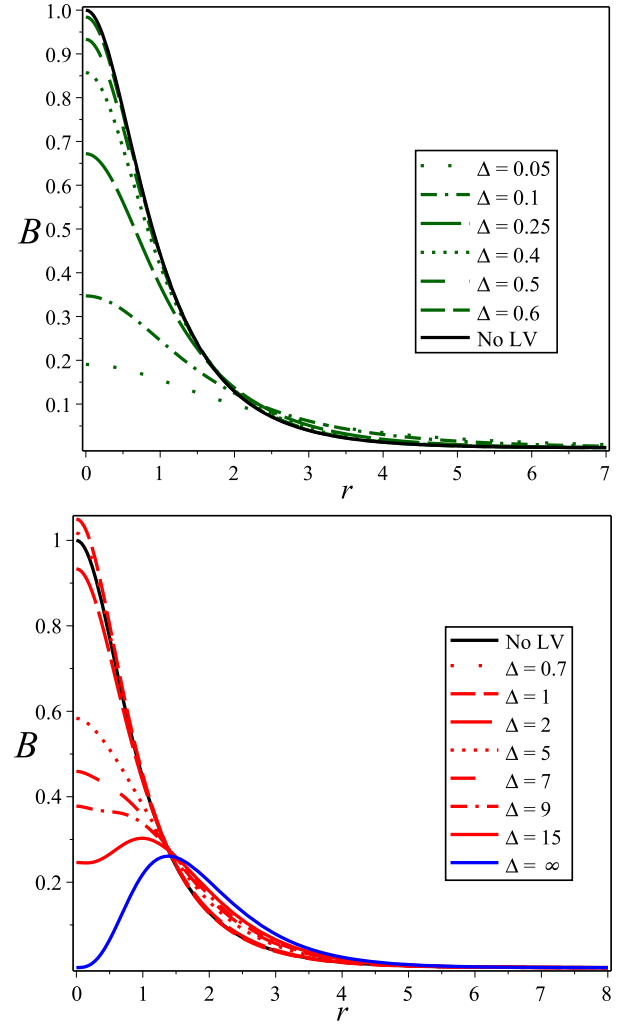


FIG. 7: The profiles of the magnetic field, $B(r)$, for winding number $n = 1$. The upper figure represents the profiles for $0 < \Delta \leq 0.642$ and the lower figure represents the profiles for $\Delta > 0.642$. The solid black line represents the profiles in the absence of Lorentz violation. The blue line is the profile for $\Delta \rightarrow \infty$.

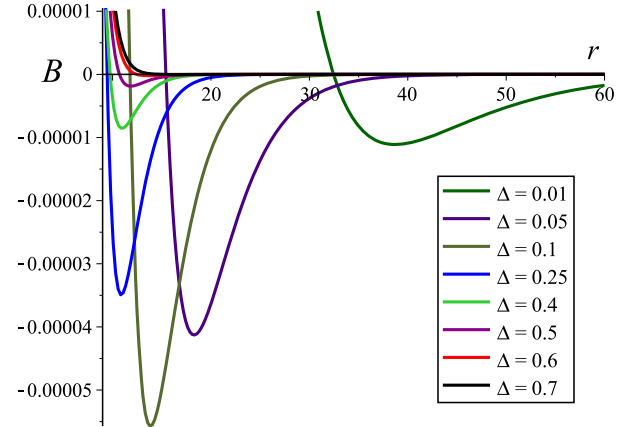


FIG. 8: Magnetic field inversion.

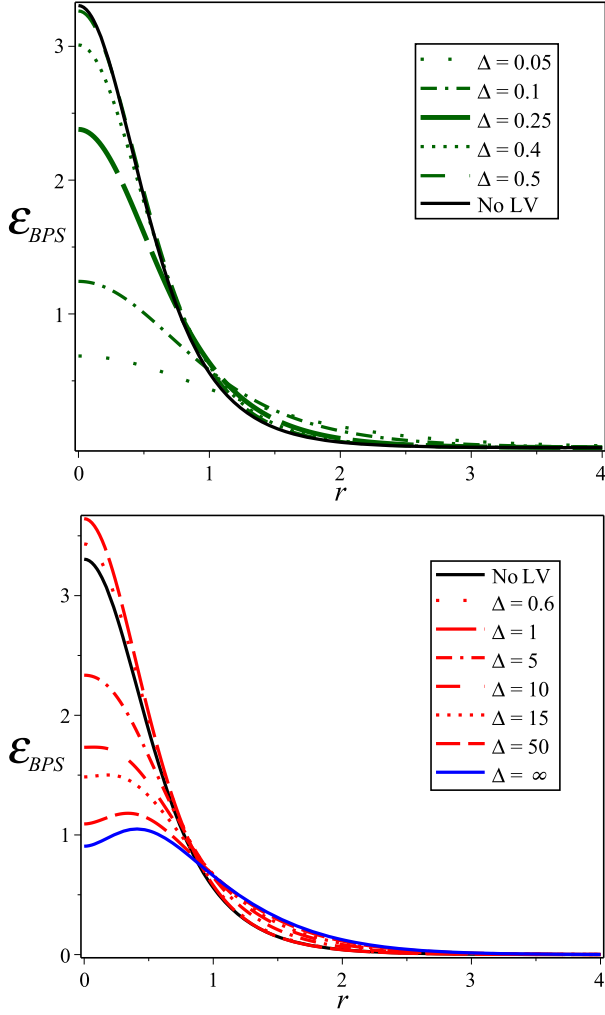


FIG. 9: The profiles of the BPS energy density, $\varepsilon_{bps}(r)$, for winding number $n = 1$. The upper figure represents the profiles for $0 < \Delta \leq 0.5$ and the lower figure represents the profiles for $\Delta \geq 0.6$. The solid black line represents the profiles in the absence of Lorentz violation. The blue line is the profile for $\Delta \rightarrow \infty$.

$1 < \Delta \lesssim 10$, the amplitude decreases while Δ increases. For $\Delta > 10$, the profiles become ringlike structures, with the behavior accentuated as Δ continuously grows. For $\Delta \rightarrow \infty$, the amplitude at the origin is ~ 0.82 (but for $n > 1$, such an amplitude is zero). Thus, for large values of Δ , the sigma model energy begins to behave as in the CSH and MCSH models, a consequence of Lorentz violation. This can be understood by analyzing the amplitude of the BPS energy density at the origin, which stems from Eq. (80),

$$\varepsilon_{BPS}(0) = \frac{4\Delta\eta^2}{(\Delta+1)^2} + \eta n^2 (G_n)^2 r^{2(n-1)}, \quad (107)$$

where it was verified that G_n is a finite quantity for any value of Δ . Then, for large values of Δ the amplitude is

$$\varepsilon_{BPS}(0) = \frac{4\eta^2}{\Delta} + \eta n^2 (G_n)^2 r^{2(n-1)}, \quad (108)$$

which for $n = 1$ becomes $\varepsilon_{BPS}(0) = \eta (G_1)^2$, a finite quantity. On the other hand, for $n > 1$, the amplitude goes to zero as quickly as Δ^{-1} does. In both cases, the numerical result is verified by the analytical analysis.

V. REMARKS AND CONCLUSIONS

We have examined a gauged $O(3)$ σ model modified by Lorentz-violating terms in the non-Abelian scalar and electromagnetic sectors, demonstrating the existence of topological self-dual configurations. In the standard gauged $O(3)$ σ model only purely magnetic self-dual configurations exist. The introduction of LV terms allows the existence of altered purely magnetic self-dual solutions and magnetic self-dual configurations carrying an electric field. Specifically, the purely magnetic self-dual configurations take place when the parity-odd, CPT -even coefficients, $(k_{\phi\phi})_{0i} = 0$, $\kappa_{0i} = 0$, are null. For $\kappa_{0i} \neq 0$, the self-dual configurations also carry an electric field but a null total electric charge. Implementing the BPS procedure, the total energy of the self-dual configurations in both cases was evaluated, revealing itself to be proportional to the topological charge of the model and to the LV coefficients introduced in the σ sector. It was noticed that, while the purely magnetic configurations were quantitatively altered in their widths by the LV terms, the charged configurations may undergo sensitive qualitative modification by the same terms, approaching the magnetic and energy behavior of the CSH and MCSH models. Furthermore, also reported was the remarkable possibility of magnetic flux reversion, which finds an application in some condensed matter systems. Therefore, we stress that the Lorentz violation significantly enriches the space of self-dual configurations found in the sigma model of Ref. [16].

Acknowledgments

R. C. and M. M. F. Jr are grateful to CNPq (Conselho Nacional de Desenvolvimento Científico e Tecnológico), CAPES (Coordenação de Aperfeiçoamento de Pessoal de Nível Superior) and FAPEMA (Fundação de Amparo à Pesquisa e ao Desenvolvimento Científico e Tecnológico do Maranhão), Brazilian funding agencies for development of science; C. F. acknowledges CAPES for the invaluable financial support.

[1] A. A. Abrikosov, Zh. Eksp. Teor. Fiz. **32**, 1442 (1957) [Sov. Phys. JETP **5**, 1174 (1957)];

[2] V. L. Ginzburg and L. D. Landau, Zh. Eksp. Teor. Fiz.

- 20, 1064 (1950); in *Collected Papers of L. D. Landau*, edited by D. Ter Haar (Pergamon Press, Oxford, 1965), p. 546.
- [3] H. Nielsen and P. Olesen, Nucl. Phys. **B 61**, 45 (1973).
- [4] S. Deser, R. Jackiw, and S. Templeton, Ann. Phys. (N.Y.) **140**, 372 (1982); G. V. Dunne, Aspects of Chern-Simons Theory, arXiv:hep-th/9902115.
- [5] R. Jackiw and E. J. Weinberg, Phys. Rev. Lett. **64**, 2234 (1990); R. Jackiw, K. Lee, and E. J. Weinberg, Phys. Rev. D **42**, 3488 (1990); J. Hong, Y. Kim, and P. Y. Pac, Phys. Rev. Lett. **64**, 2230 (1990); G. V. Dunne, *Self-Dual Chern-Simons Theories* (Springer, Heidelberg, 1995).
- [6] C.k. Lee, K. M. Lee, and H. Min, Phys. Lett. B **252**, 79 (1990).
- [7] A. A. Belavin and A. M. Polyakov, JETP Lett. **22**, 245 (1975).
- [8] R. Rajaraman, *Solitons and Instantons* (North-Holland, Amsterdam 1982); W. J. Zakrzewski, *Low Dimensional Sigma Models* (Hilger, Bristol, England, 1989).
- [9] E. B. Bogomol'nyi, Sov. J. Nucl. Phys. **24**, 449 (1976); M. K. Prasad and C. M. Sommerfield, Phys. Rev. Lett. **35**, 760 (1975).
- [10] R. A. Leese, M. Peyrard, and W. J. Zakrzewski, Nonlinearity **3**, 387 (1990).
- [11] M. Peyrard, B. M. A. G. Piette, and W. J. Zakrzewski, Nonlinearity **5**, 563 (1992).
- [12] R. A. Leese, Nucl. Phys. **B344**, 33 (1990); Nucl. Phys. **B366**, 283 (1991).
- [13] B. J. Schroers, Phys. Lett. B **356**, 291 (1995).
- [14] P. K. Ghosh and S. K. Ghosh, Phys. Lett. B **366**, 199 (1996).
- [15] P. Mukherjee, Phys. Lett. B **403**, 70 (1997).
- [16] P. Mukherjee, Phys. Rev. D **58**, 105025 (1998).
- [17] F. S. A. Cavalcante, M. S. Cunha, and C. A. S. Almeida, Phys. Lett. B **475**, 315 (2000); M. S. Cunha, R. R. Landim and C. A. S. Almeida, Phys. Rev. D **74**, 067701 (2006).
- [18] D. Bazeia, E. da Hora, R. Menezes, H. P. de Oliveira, and C. dos Santos, Phys. Rev. D **81**, 125016 (2010); D. Bazeia, E. da Hora, C. dos Santos, and R. Menezes, Phys. Rev. D **81**, 125014 (2010); D. Bazeia, E. da Hora, and R. Menezes, Phys. Rev. D **85**, 045005 (2012).
- [19] D. Colladay and V. A. Kostelecky, Phys. Rev. D **55**, 6760 (1997); **58**, 116002 (1998).
- [20] S. R. Coleman and S. L. Glashow, Phys. Rev. D **59**, 116008 (1999).
- [21] F. R. Klinkhamer and M. Schreck, Nucl. Phys. **B848**, 90 (2011); M. Schreck, Phys. Rev. D **86**, 065038 (2012); M. A. Hohensee, R. Lehnert, D. F. Phillips, and R. L. Walsworth, Phys. Rev. D **80**, 036010 (2009); A. Moyotl, H. Novales-Sánchez, J. J. Toscano, and E. S. Tututi, Int. J. Mod. Phys. A **29**, 1450039 (2014); **29**, 1450107 (2014); M. Cambiaso, R. Lehnert, and R. Potting, Phys. Rev. D **90**, 065003 (2014); R. Bufalo, Int. J. Mod. Phys. A **29**, 1450112 (2014).
- [22] V. A. Kostelecky, Phys. Rev. D **69**, 105009 (2004); R. Bluhm and V. A. Kostelecky, Phys. Rev. D **71**, 065008 (2005); Q. G. Bailey and V. A. Kostelecky, Phys. Rev. D **74**, 045001 (2006); C. Hernaski, Phys. Rev. D **90**, 124036 (2014); R. V. Maluf, J. E. G. Silva, and C. A. S. Almeida, Phys. Lett. B **749**, 304 (2015).
- [23] V. A. Kostelecky and C. D. Lane, J. Math. Phys. (N.Y.) **40**, 6245 (1999); R. Lehnert, J. Math. Phys. (N.Y.) **45**, 3399 (2004); D. Colladay and V. A. Kostelecky, Phys. Lett. B **511**, 209 (2001); T. Mariz, J. R. Nascimento, and A. Yu. Petrov, Phys. Rev. D **85**, 125003 (2012); G. Gazzola, H. G. Fargnoli, A. P. Baeta Scarpelli, M. Sampaio, and M. C. Nemes, J. Phys. G **39**, 035002 (2012); A. P. Baeta Scarpelli, M. Sampaio, M. C. Nemes, and B. Hiller, Eur. Phys. J. C **56**, 571 (2008); F. A. Brito, L. S. Grigorio, M. S. Guimaraes, E. Passos, and C. Wotzasek, Phys. Rev. D **78**, 125023 (2008); F. A. Brito, E. Passos, and P. V. Santos, Europhys. Lett. **95**, 51001 (2011); C. F. Farias, A. C. Lehum, J. R. Nascimento, and A. Yu. Petrov, Phys. Rev. D **86**, 065035 (2012); J. R. Nascimento, A. Yu. Petrov, C. Wotzasek, and C. A. D. Zarro, Phys. Rev. D **89**, 065030 (2014); O. M. Del Cima, J. M. Fonseca, D. H.T. Franco, O. Piguet, Phys. Lett. B **688**, 258 (2010). R. V. Maluf, J. E. G. Silva, W. T. Cruz, and C. A. S. Almeida, Phys. Lett. B **738**, 341 (2014).
- [24] V. A. Kostelecky, C. D. Lane, A. G. M. Pickering, Phys. Rev. D **65**, 056006 (2002); C. D. Carone, M. Sher, M. Vanderhaeghen, Phys. Rev. D **74**, 077901 (2006); W. F. Chen, G. Kunstatter, Phys. Rev. D **62**, 105029 (2000); O. M. Del Cima, D. H. T. Franco, A. H. Gomes, J. M. Fonseca, O. Piguet, Phys. Rev. D **85**, 065023 (2012); T. R. S. Santos, R. F. Sobreiro, Phys. Rev. D **91**, 025008 (2015).
- [25] S. M. Carroll, G. B. Field, and R. Jackiw, Phys. Rev. D **41**, 1231 (1990).
- [26] V. A. Kostelecky and M. Mewes, Phys. Rev. Lett. **87**, 251304 (2001); Phys. Rev. D **66**, 056005 (2002); Phys. Rev. Lett. **97**, 140401 (2006).
- [27] B. Altschul, Nucl. Phys. **B796**, 262 (2008); Phys. Rev. Lett. **98**, 041603 (2007); C. Kaufhold and F. R. Klinkhamer, Phys. Rev. D **76**, 025024 (2007).
- [28] F. R. Klinkhamer and M. Risse, Phys. Rev. D **77**, 016002 (2008); **77**, 117901 (2008); F. R. Klinkhamer and M. Schreck, Phys. Rev. D **78**, 085026 (2008).
- [29] M. Cambiaso, R. Lehnert, and R. Potting, Phys. Rev. D **85**, 085023 (2012); B. Agostini, F. A. Barone, F. E. Barone, P. Gaete, and J. A. Helayël-Neto, Phys. Lett. B **708**, 212 (2012); L. Campanelli, Phys. Rev. D **90**, 105014 (2014); R. Bufalo, B. M. Pimentel, and D. E. Soto, Phys. Rev. D **90**, 085012 (2014).
- [30] R. C. Myers and M. Pospelov, Phys. Rev. Lett. **90**, 211601 (2003); C. M. Reyes, L. F. Urrutia, and J. D. Vergara, Phys. Rev. D **78**, 125011 (2008); Phys. Lett. B **675**, 336 (2009); C. M. Reyes, Phys. Rev. D **82**, 125036 (2010); **80**, 105008 (2009); **87**, 125028 (2013); C. M. Reyes, S. Ossandon, and C. Reyes, Phys. Lett. B **746**, 190 (2015).
- [31] M. A. Anacleto, F. A. Brito, and E. Passos, Phys. Rev. D **86**, 125015 (2012); M. A. Anacleto, Phys. Rev. D **92**, 085035 (2015); E. O. Silva and F. M. Andrade, Europhys. Lett. **101**, 51005 (2013); F. M. Andrade, E. O. Silva, T. Prudêncio and C. Filgueiras, J. Phys. G **40** 075007 (2013).
- [32] K. Bakke and H. Belich, J. Phys. G **39**, 085001 (2012); K. Bakke, H. Belich, and E. O. Silva, J. Math. Phys. (N.Y.) **52**, 063505 (2011); J. Phys. G **39**, 055004 (2012); K. Bakke and H. Belich, J. Phys. G **39**, 085001 (2012); Ann. Phys. (N.Y.) **333**, 272 (2013); A. G. de Lima, H. Belich, and K. Bakke, Ann. Phys. (Berlin) **526**, 514 (2014); Eur. Phys. J. Plus **128**, 154 (2013).
- [33] M. N. Barreto, D. Bazeia, and R. Menezes, Phys. Rev. D **73**, 065015 (2006); A. de Souza Dutra, M. Hott, and F. A. Barone, Phys. Rev. D **74**, 085030 (2006); D. Bazeia, M. M. Ferreira, Jr., A. R. Gomes, R. Menezes, Physica

- (Amsterdam) **239D**, 942 (2010); A. de Souza Dutra and R. A. C. Correa, Phys. Rev. D **83**, 105007 (2011); R. A. C. Correa, R. da Rocha, A. de Souza Dutra, Ann. Phys. **359**, 198 (2015).
- [34] N. M. Barraz, Jr., J. M. Fonseca, W. A. Moura-Melo, and J. A. Helayel-Neto, Phys. Rev. D **76**, 027701 (2007); A. P. Baeta Scarpelli and J. A. Helayel-Neto, Phys. Rev. D **73**, 105020 (2006).
- [35] M. D. Seifert, Phys. Rev. Lett. **105**, 201601 (2010); Phys. Rev. D **82**, 125015 (2010).
- [36] A. de Souza Dutra and R. A. C. Correa, Adv. High Energy Phys. **2015**, 673716 (2015).
- [37] R. A. C. Correa, Roldao da Rocha, A. de Souza Dutra, Phys. Rev. D **91**, 125021 (2015).
- [38] C. Miller, R. Casana, M. M. Ferreira, Jr., and E. da Hora, Phys. Rev. D **86**, 065011 (2012).
- [39] R. Casana, M. Ferreira, Jr., E. da Hora, and C. Miller, Phys. Lett. B **718**, 620 (2012).
- [40] L. Sourrouille, Phys. Rev. D **89**, 087702 (2014); R. Casana and L. Sourrouille, Phys. Lett. B **726**, 488 (2013).
- [41] C. H. Coronado Villalobos, J. M. Hoff da Silva, M. B. Hott, and H. Belich, Eur. Phys. J. C **74**, 2799 (2014).
- [42] H. Belich, F. J. L. Leal, H. L. C. Louzada, and M. T. D. Orlando, Phys. Rev. D **86**, 125037 (2012).
- [43] R. Casana and G. Lazar, Phys. Rev. D **90**, 065007 (2014).
- [44] K. Kimm, K. Lee, and T. Lee, Phys. Rev. D **53**, 4436 (1996); J. Han and H.-S. Nam, Lett. Math. Phys. **73**, 17 (2005).
- [45] S. Bolognesi and S. B. Gudnason, Nucl. Phys. **B805**, 104 (2008).
- [46] B.-H. Lee, C.-k. Lee, and H. Min, Phys. Rev. D **45**, 4588 (1992).
- [47] E. Witten and D. Olive, Phys. Lett. **78B**, 97 (1978).
- [48] E. Babaev, J. Jäykkä, and M. Speight, Phys. Rev. Lett. **103**, 237002 (2009).